Published in final edited form as:
Biopolymers. 2009 May ; 91(5): 340–350. doi:10.1002/bip.21136.

FtsZ Condensates: An In Vitro Electron Microscopy Study

David Popp[1], **Mitsusada Iwasa**[1], **Akihiro Narita**[2], **Harold P. Erickson**[3], and **Yuichiro Maéda**[1,2]

[1]ERATO "Actin Filament Dynamics" Project, Japan Science and Technology Corporation, c/o RIKEN Harima Institute at Spring 8, 1-1-1 Kouto, Sayo, Hyogo 679-5148, Japan

[2]Division of Biological Sciences, Structural Biology Research Center and Furo-Cho, Nagoya University Graduate School of Science, Chikusa-ku, Nagoya 464-8601, Japan

[3]Department of Cell Biology, Duke University Medical Center, Durham, NC 27710

Abstract

In vivo cell division protein FtsZ from E. coli forms rings and spirals which have only been observed by low resolution light microscopy. We show that these suprastructures are likely formed by molecular crowding which is a predominant factor in prokaryotic cells and enhances the weak lateral bonds between proto-filaments. Although FtsZ assembles into single proto-filaments in dilute aqueous buffer, with crowding agents above a critical concentration, it forms polymorphic supramolecular structures including rings and toroids (with multiple protofilaments) about 200 nm in diameter, similar in appearance to DNA toroids, and helices with pitches of several hundred nm as well as long, linear bundles. Helices resemble those observed in vivo, whereas the rings and toroids may represent a novel energy minimized state of FtsZ, at a later stage of Z-ring constriction. We shed light on the molecular arrangement of FtsZ filaments within these suprastructures using high resolution electron microscopy.

Keywords

FtsZ; molecular crowding; multivalent cations; supramolecular structures; toroid; helices

INTRODUCTION

In both eukaryotic and prokaryotic cells, cytoskeletal proteins are likely to assemble in vivo into structures with a thickness greater than a single molecule and the formation of lateral interactions between individual filaments and their regulation may have important consequences for understanding filament assembly and function. Within the cell, these supramolecular structures arise mainly due to short-range forces as a consequence of molecular crowding (up to 40% of the cells volume is occupied by various proteins) as well as cytoskeletal binding proteins. An example of suprastructures formed in eukaryotic cells is the actin cytoskeleton, where parallel actin bundles have been observed near the cell surface in lamellopodia or filapodia.[1]

One of the best studied in vitro system of supramolecular condensates experimentally and theoretically is DNA, which also exists in highly condensed, tightly packed states in viruses

Correspondence to: David Popp; e-mail: dpopp@spring8.or.jp .

and sperm cells in vivo.[2] The principle morphologies of these structures are toroids, spheroids, and rod-like, and these condensates were extensively investigated in vitro.

Cell division protein FtsZ, a microtubule homolog assembles at mid-cell into a ring called the Z-ring. The ring forms on the inside of the cytoplasmic membrane and mediates membrane constriction, resulting in the production of two newborn cells. The Z-rings donut- or toroid-like appearance has been observed by fluorescent light microscopy (FLM) techniques,[3,4] yet it has never been observed by direct in vivo electron microscopy. In a recent study by cryo-electron tomography, the structure of the ring appeared to comprise short protofilaments scattered around the location of the ring, but with no obvious lateral bonds or connections.[5] The Z-ring is highly dynamic, continually remodeling itself before and after its constriction, with a halftime turnover of about 8 s[6]. Subunit exchange in the Z-ring depends on GTP hydrolysis.[6] Recently, it has been shown by FLM that in addition to forming a Z-ring at the division site, FtsZ also forms dynamic helical-like assemblies in vegetatively growing wildtype cells of *B. subtilis*.[7] This helical-like localization pattern occurred prior and independently to Z-ring formation. Spiral-like patterns of FtsZ have also been observed in exponentially growing *E. coli* cells[8] and it has been proposed that upon disassembly of the Z-ring, FtsZ is redistributed in a dynamic helical cytoskeleton. It was suggested that this dynamic helix created a reservoir for the rapid turnover of FtsZ in the Z ring.[8] As the resolution of FLM is only in the range of 0.25 μm, nothing is known how FtsZ filaments are arranged in the supramolecular structures of the Z-ring and the helices at a molecular level. Here, we shed light on this issue, by showing that both ring-like and helical structures of FtsZ similar to those observed in vivo can be induced in vitro by crowding agents and their molecular structures, supra-structures, and interfilament interactions visualized by high-resolution electron microscopy.

Usually, multivalent cations also allow biopolymers to condense into suprastructures, which for DNA (toroids)[2] or actin (bundles)[9] have been shown to be similar to those formed by molecular crowding. Multivalent cations have not been extensively tested on FtsZ in the past and only the effect of Ca^{2+} ions have been described, which led to crystalline sheets or helical tubes.[10] Here, we investigated for the first time FtsZ condensates formed by other multivalent cationslike Hexammine Cobalt. We found that *E. coli* FtsZ is a unique biopolymer in the sense that condensates formed by molecular crowding and cations are entirely distinct. Furthermore, we observed novel arrangements of FtsZ molecules in the proto-filaments in some of the crystalline structures formed by Hexammine Cobalt, which differ from those described for Ca^{2+} induced sheets.[10] They also differed from the arrangement of FtsZ filaments in the bundled or toroid structures, we observed when formed by molecular crowding, which appeared to be skewed, rather than straight proto-filaments.

MATERIALS AND METHODS

Chemicals

All chemicals used were from SIGMA, except methyl cellulose (MC) which was from WAKO and polyvinyl alcohol (PVA) which was purchased from Kanto Chemical Co.

Buffers and Experimental Procedures

Wild-type FtsZ was expressed and purified as described.[11] The protein was frozen in small aliquots in Eppendorf tubes cooled in liquid nitrogen and stored at −80°C until use. Buffers used were KMgbuffers at pH 6.6 and pH 7.7 (30 m*M* Mes, pH 6.6 or 30 m*M* Hepes, pH 7.7, 0.2 m*M* EGTA, 3 m*M* MgAc, 180 m*M* KAc, 1 m*M* DTT). NaMg-buffers contained 180 m*M* NaCl instead of KCl. We found no difference substituting MgAc by $MgCl_2$, KAc by KCl or NaAc by NaCl. Adjustment of pH was done with KOH for KMg-buffers and NaOH for NaMg buffers. In some cases, equal amounts of KCl and NaCl (90 m*M* each) were used and the pH

was adjusted by approximately equal amounts of NaOH and KOH. In some cases, $MgCl_2$ was replaced by 3 m*M* EDTA (KEDTA-buffer and NaEDTA-buffer). The buffers were chosen for the following rationales. pH 7.7 is close to the physiological pH of *E. coli* cytoplasm, but pH around 6.6 has been used for many in vitro assembly studies in the past. Assembly in the presence of Mg^{2+} ions is accompanied by GTP hydrolysis, whereas in EDTA assembly occurs but hydrolysis is completely blocked.

Before an experiment, the protein was quickly thawed and dialyzed against one of the buffers with several changes of buffer using an oscillatory micro-dialysis system (Bio Tech). In some cases, we cycled the protein through a round of Ca^{2+} assembly and disassembly to remove inactive protein as described.[11] We could not find any major differences in assembly using the additional calcium step, so we conventionally thawed and dialyzed FtsZ, which was subjected to a short high-speed centrifugation step just before the experiment to remove any possible aggregates. The protein was stored on ice and used within 2 days. The protein concentration was determined using a BCA assay and corrected for the 75% color ratio of FtsZ/BSA.[11] ZipA189-328 was expressed and purified as described.[12]

Preparation of FtsZ Suprastructures and Electron Microscopy

Monomeric FtsZ was mixed with the appropriate amount of crowding agent at 25°C (final FtsZ concentration was mostly 12.5 μM) and polymerization was induced by addition of nucleotide to a final concentration of 2 m*M*. After 3–5 min, a drop of protein solution was applied to carbon-coated, glow-discharged copper grids, blotted, and stained with 2% uranylacetate and air dried and visualized under a Jeol JEM-2010 HC microscope operated at 100 keV and a nominal magnification between 8000 and 60,000. Experiments with multivalent cations were done as follows: FtsZ was dialyzed against low salt buffers (no NaCl or KCl present), pH 7.7. Multivalent cations (2 m*M* Hexammine Cobalt, 5 m*M* spermine, 5 m*M* $BaCl_2$) final concentrations were mixed with FtsZ monomers (final concentation 25–75 μM) and nucleotide (2 m*M*) was added at 258C. Suspensions were left at room temperature for 30 min. Crystalline sheets and other structures formed with Hexammine Cobalt were collected by very brief (few seconds) low-speed centrifugation and resuspended in buffer, applied to EM grids blotted washed with a drop of buffer, and stained with 2% uranyl acetate. With Hexammine Cobalt, addition of salt usually resulted in smaller sheets or tubes. FtsZ-ZipA tubes were prepared as follows: first FtsZ-ZipA complex was formed by adding excess amount (10%) of ZipA to FtsZ, then Hexammine Cobalt (2 m*M*) and GTP (2 m*M*) were added and the precipitated material collected after 30 min, resuspended in buffer and applied to grids and stained. In the tubes formed FtsZ was in a complex with ZipA as judged from SDS gels of precipitated material briefly centrifuged and washed several times (supp. info., Figure 5c).

Films were digitized with PhotoScan2000 (Z/I Imaging) at 7μm steps and Fourier transforms and averaged filtered images were calculated using the EM computing package recently described.[13] Otherwise, electron micrographs were scanned at 1200 dpi on an Epson scanner and displayed by Image J and Photoshop. Analysis of toroid sizes and parameters of helical suprastructures-like pitch and amplitude was done by hand using Image J.

RESULTS

First, we describe the effects of molecular crowding leading to *Escheria coli* FtsZ suprastructures. In vitro, we mixed various amounts of crowding agents (CA's) such as PVA, MC, or Ficoll 70 with FtsZ monomers. After adding nucleotide, we observed the polymer structures formed under the electron microscope.

For most experiments, the final concentration of FtsZ was kept constant at 12.5 μM. Below a critical concentration, c_0 of crowding, which varied between the different crowding agents

used (about 0.75% MC, 3% PVA, 30% Ficoll 70), FtsZ formed mostly single filaments, with few filaments forming lateral interactions leading to doublets (Figure 1a). We have previously shown that the FtsZ filaments steady state length distribution under these conditions was a tightly coupled double exponential[14] with an average filament length ⟨L⟩ of about 180 nm. It should be noted that c_0 depends on the concentration of FtsZ used; it decreased when the protein concentration was higher, and likewise more crowding agent was needed to form suprastructures when the FtsZ concentration was lower due to the excluded volume effect. This is a general principle of molecular crowding[15] and has also been described recently for actin nematic liquid crystal and bundle formation under crowded conditions.[16]

Above the critical concentration, c_0 of crowding agents, the equilibrium of single filaments was shifted dramatically to structures consisting of more than one filament. Independent of the pH (we probed pH 6.6 and pH 7.7) and in the presence of potassium and magnesium ions (180 m*M* KAc or KCl, 3 m*M* MgAc or $MgCl_2$, KMg-buffer) the main structures of FtsZ observed were rings made from multiple individual filaments with an average diameter of about 240 nm (Figure 1b, supp. info., Figure 1a). In the following, for reasons of simplicity, we will call these structures 200 nm rings.

Increasing the crowding agent concentration further led to highly condensed rings and the formation of well-defined toroids (Figure 1c). The formation of rings or toroids with an inner diameter (a) and an outer diameter (b) (supp. info., Figure 1) was independent of the nucleotide used and could be observed with GTP (Figure 1b, supp. info., Figure 2a) as well as with nonhydrolysable nucleotides GMPPNP (Figure 1c) or GTPγS (supp. info., Figure 2b) but not with GDP (supp. info., Figure 2c), which only formed amorphous polymers in the presence of crowding agents. Yet the inner diameter (a) and outer diameter (b) of well condensed toroids could vary with the bound nucleotide, being largest for GTP and smallest for GTPγS (supp. info., Figures 1b and 1c).

The architecture of toroids was difficult to establish as they were large densely packed structures, which usually appeared like swim rings with a thickness and heights of about 200 nm (Figure 1c). Yet, we could learn about the arrangement of FtsZ filaments by studying loosely condensed rings just above c_0. At high magnification, it became obvious that these rings did not consist of only one long annealed FtsZ filament wrapped into circles, but of many individual single FtsZ filaments, which made lateral contacts between their neighbors (Figure 1d). In most cases, the rings appeared to be formed by FtsZ filaments larger than a single filament (supp. info., Figure 1d). We compared the diameter of FtsZGTP rings consisting of only several turns to the inner diameter of fully condensed FtsZ-GTP toroids and found both values to be rather similar, indicating that as more and more FtsZ filaments condensed with increasing crowding agent concentration, the toroids mostly grew to the outside, but not to the inside (supp. info., Figure 1). The filament length of FtsZ filaments forming a ring was mostly larger than the average filament length ⟨L⟩ of 180 nm observed below c_0. Many filaments appeared to be around 400–800 nm long, forming about one turn of the 200 nm ring. This may imply that end-to-end annealing became more favorable under crowded conditions.

Loosely condensed rings with a diameter of 500 nm were also observed (supp. info., Figure 3a), and in few cases, the inner diameter of toroids was only about 100 nm. Although rings and toroids were the main species observed under these conditions, other supramolecular structures also formed. Helices formed by multiple filaments with a pitch of about 300 nm and an amplitude around 150 nm (Figure 2a) as well as long straight FtsZ bundles (Figure 2b) coexisted with rings and toroids. Optical diffraction patterns from bundles consistently showed two major reflections (Figure 2c), an equatorial reflection at about 59 Å arising from the packing of adjacent filaments and an off meridional reflection at about 44 Å. In toroids, some regions showed an equatorial peak at about 58 Å indicating that the interfilament spacing was similar

to that in straight bundles (supp. info., Figure 2e). Yet, some areas within toroids did not give rise to any reflection. In no case could we observe a clear higher-order equatorial reflection arising from a hexagonal packing, indicating that the packing is more liquid-like and the order is far better preserved overall in the straight FtsZ bundles than in the toroids, where the interparticle spacing is only well defined in some areas. Negative stain has been shown to fix biological fibrous proteins on the millisecond timescale retaining their structure[17] yet subsequent drying usually leads to a shrinkage and flattening of the structures by several percent.[17] Therefore, the interfilament packing could be a bit larger in the native state than measured here.

Effects of EDTA

Next, we investigated the assembly of FtsZ in the presence of EDTA and crowding agents above c_0 in KEDTA buffer. EDTA blocks GTP hydrolysis and should give an assembly reaction that is not complicated by any reversible hydrolysis step. At pH 7.7 rings, toroids, short helices, and long tube-like toroid coexisted (supp. info., Figure 3b). Yet, at pH 6.6, the equilibrium was almost completely shifted to long helices (Figure 3a). No other major supramolecular structures were formed under these conditions. The helices were remarkably regular, with a very long pitch around 780 nm and a height of about 260 nm (Figure 3b, Table I). The same predominant helical supramolecular structures were observed when GTP was replaced by GMPPNP. These helices formed even in the absence of potassium ions, indicating that shielding the negative charge of FtsZ filaments is not necessary to form these suprastructures (supp. info. Figure 3c). This is not surprising as like charge attractions have been observed in a variety of systems[18] arising from dynamic "van der Waals"-like correlations of long-wavelength ion fluctuations.[19]

Under low salt conditions, helices were not always fully condensed in some areas which allowed us to examine the architecture of these structures (Figure 3c). We were able to track individual filaments in the loosely packed areas and most filaments appeared to be at least 2–3 μm long, again indicating that annealing under crowded conditions may be a more favored reaction than in aqueous solutions. Adding GTPγS to FtsZ in KEDTA buffer resulted in long straight bundles (supp. info., Figure 3d) indicating that GTPγS binding affects the FtsZ polymer in different and more complicated ways than GMPPNP. In the following, we have concentrated more on FtsZ supramolecular formed in the presence of GTP and GMPPNP.

Effects of Sodium Ions

We further probed for other polymorphic structures of FtsZ in a crowded environment above c_0 by replacing potassium with sodium ions as it is known that some bacteria also contain sodium pumps which drive the motion of flagella. Interestingly, the resulting suprastructures differed from those formed in the presence of potassium ions. With sodium ions (200 m*M* NaAc or NaCl), magnesium ions (3 m*M* MgAc or $MgCl_2$), and GTP present (NaMg-buffer), rings and toroids, which were the majority species in the presence of potassium ions were not predominant. Instead and independent of the pH mainly helical suprastructures multiple filament wide with a pitch of about 390 nm and an amplitude of around 130 nm formed (Figure 4a, Table I). Replacing magnesium by EDTA (NaEDTA-buffer) resulted in larger condensed supramolecular structures which appeared to be helical at first glance (Figure 4b), yet higher resolution images showed that these structures could be described as planar waves (Figure 4c). These wave structures, with a pitch of about 330 nm and amplitude around 130 nm, could be several μm wide (Figure 4d, Table I). Probably the large width of these spindleshaped aggregates prevented them from forming a spiral.

In the presence of equal amount of sodium and potassium ions, the regular structures we observed in the presence of sodium and potassium ions alone were only formed locally, whereas

in most parts the suprastructures were large tightly interwoven tubes or toroids with irregular appearance (supp. info., Figure 4).

Effects of Multivalent Cations

Now, we turn to the effect of multivalent cations. It is a well-known phenomena that other biological polymers like Factin and DNA collapse into higher-ordered structures by the addition of polycations.[2,9] DNA has been shown to form mainly toroids not only by the addition of crowding agents but also by multivalent cations such as Hexammine Cobalt, spermine, or barium chloride.[2] This striking similarity of FtsZ and DNA toroids (see Figure 8 in Ref. 2) led us to perform polymerization experiments of FtsZ in the presence of multivalent cations. We found that the suprastructures formed by the multivalent cations were entirely distinct from those formed by crowding agents, which differs completely from DNA[2] or actin[9] condensation, where similar structures were formed both with crowding agents and cations.

In the presence of Hexammine Cobalt, magnesium, and nucleotide, FtsZ formed large crystalline sheets (Figure 5a), which could be over 1 μm long and several hundred μm wide. The best ordered and larger sheets were obtained with GTP rather than GMPPNP and the optical diffraction from FtsZ-GTP sheets gave a set of discrete crystalline reflections (Figure 5a, insert), which were used to calculate an averaged filtered image. Single FtsZ protofilaments were arranged parallel to each other in the direction of the long dimension of the crystal (Figure 5b).

Exchanging magnesium to EDTA led to different morphologies in the presence of Hexammine Cobalt depending on the nucleotide. In the presence of GTP mainly long helical ribbons formed (Figure 5d), in the presence of GMPPNP, we observed helical tubes (Figure 5e), whereas with GDP several μm long and up to 500 nm wide crystalline tubes (as judged from their sharp optical diffraction patterns)were predominant (Figure 5c).

In the presence of other multivalent cations like spermine or barium chloride, thin sheets or rolled up sheets were observed (see Figure 6). Whereas the spermine-induced suprastructures did not give rise to a clear optical diffraction pattern, $BaCl_2$ induced thin bundles consistently showed a pair of reflections, one an off meridional reflection at about 45 Å and a weak but clearly visible true meridional reflection at about 42 Å (Figure 6b).

DISCUSSION

Recently studies have established that *E. coli* FtsZ could assemble into rings in the absence of all other known bacterial proteins[20] and *E. coli* FtsZ could also be assembled into rings of about 500 nm diameter in fission yeast cells.[4] Presumably in the latter case, the bacterial cell diameter established the initial diameter of the FtsZ ring due to the attractive potential of the membrane leading to short-range forces on fibrous proteins as has been predicted by the DLVO-theory in the past.[21] In addition to forming a Z-ring, FtsZ also formed dynamic transient helical assemblies. Depending on distinct stages of the cell cycle three different localization patterns of FtsZ leading to cytokinesis were identified. In newborn cells, FtsZ moved in helical patterns over the whole length of the cell and as time progressed this helix became shorter and redistributed into a ring structure.[7] The structural relationship between FtsZ spirals and Z-rings has not been established. Also, not much is known about structural details like interfilament interactions of these supramolecular structures, as in vivo cryoelectron microscopy studies were only able to visualize fragments of the Z-ring and no helical FtsZ spirals have been observed.[5] Our in vitro EM observations is the first conclusive high resolution study showing that similar structures as observed in vivo, may be mainly a result of molecular crowding. Important factors governing which polymorphic state FtsZ filaments may adopt in a crowded

environment, helical, ring, or wave-like were largely dependant are magnesium, potassium, and sodium ions.

On the other hand, GTP hydrolysis did not seem to have a large effect on the final suprastructure, as filaments assembled in the presence of crowding agents and GTP under various conditions were very similar to those assembled with the nonhydrolysable nucleotide GMPPNP. Filaments assembled by GTPγS could differ as they assumed a straight configuration instead of spirals in KEDTA buffer. In aqueous buffers lacking crowding agents, GTPγS was not capable of inducing any FtsZ polymerization at all.[22] Therefore, it was a new finding that in the presence of crowding agents GTPγS could form FtsZ polymers and condense into ring-like or straight bundled suprastructures. Yet GMPPNP was a better substrate than GTPγS as we observed similar suprastructures with both GTP and GMPPNP. This finding supports results, which suggested that the majority of FtsZ within protofilaments has GTP bound rather than GDP.[23] Previous in vitro studies[24–27] suggested that FtsZ in the GTP bound state predominantly formed straight protofilaments, whereas GDP bound FtsZ formed curved protofilaments. Yet most of these studies were done in the presence of high amounts of Ca^{2+} ions or highly positively charged substances like DEAEdextran, conditions which are far from physiological. Our results did not support this conclusion, as in most cases, we observed curved configurations of FtsZ in the form of rings and spirals in the presence of GTP, it's nonhydrolysable analog GMPPNP and crowding agents, whereas with GDP FtsZ only formed irregular polymorphic aggregates in the presence of crowding agents.

Another interesting finding was that when Mg^{2+} ions were chelated by EDTA long spirals formed especially at lower pH of 6.6, rather than rings or toroids which were the majority species in the presence of Mg^{2+}. It is likely that Mg^{2+} was stripped from the bound nucleotide by EDTA, as the magnesium ion was not always seen in FtsZ crystal structures. Thus the presence or absence of magnesium may trigger a structural change of the FtsZ monomer itself or affect the binding site between subunits, which in turn could lead to the observed different supramolecular structures.

Our in vitro results provide evidence, that both the Z-ring and spiral structures observed in vivo,[4,7,8] arise mainly from the cells molecular crowding (30–40% of the prokaryotic cytoplasm is filled with various proteins). It also supports the idea that one type of polymer is directly derived from the other, so that FtsZ molecules arranged in longer helices can transform into helices with a shorter pitch and subsequently the ring perhaps by small changes in the environment.[7] The maximum ring sizes we observed had a diameter around 500 nm which is similar to toroids observed recently in vivo[4] and is in the range of several bacterial species, which have a diameter of about 500 nm at the Z-ring position. Yet the majority of rings had a diameter of about 200 nm, which suggests that this state is an energy minimum, perhaps at a later point of Z-ring constriction. Few toroids had an even smaller diameter of only 100 nm. The helical filaments, we observed had pitches between about 300 and 800 nm, which was in the same range as the spirals observed in vivo.[7] Whether the helices were left or right handed could not be determined from the EM projections with accuracy. All supramolecular structures were made up from multiple FtsZ filaments which associated laterally and many filaments were longer than the average filament length found in aqueous solutions which was most likely induced by end-to-end annealing. If the FtsZ filaments within the 3-D suprastructures are arranged parallel, antiparallel, or random cannot be determined at present. For the bacterial segregation protein ParM which also formed condensates under various conditions, we could show that the lateral interaction sites for parallel or antiparallel binding were rather similar, thus leading to a random orientation of filaments in the bundles or rafts formed (Popp et al., in preparation). One may speculate that FtsZ filaments may behave similarly in the absence of associated proteins, as FtsZ filaments were found to be arranged in both parallel or antiparallel configurations in 2-D sheets described in the literature.[10,26]

Fully condensed toroids showed regions where the spacing between FtsZ filaments although liquid-like was regular. How is the architecture of FtsZ toroids related to the wellstudied DNA toroids which they closely resemble? In DNA toroids, the DNA is circumferentially wound around the toroid much like one would coil a length of rope and in many regions packed in a hexagonal lattice.[2] The first step in DNA toroid formation is the spontaneous formation of a nucleation loop, which acts as a nucleation site for condensation on which the remainder of the DNA polymer condenses to form a proto-toroid. This proto-toroid then grows equally inward and outward by the addition of free DNA polymers from the solution. A similar mechanism seems likely for FtsZ condensation under crowded conditions, yet opposed to DNA toroids, FtsZ toroids grew mainly outward, which again indicates that the 200 nm ring diameter is an energetically favored state.

Another finding in this study is that the 200 nm ring structure was closely associated with potassium ions, whereas spirals and planar waves were generally observed in the presence of sodium ions. Why sodium and potassium ions induce different polymorphic structures of FtsZ remains unknown at present.

In general, the cytoplasm of *E. coli* contains high amount of potassium ions over 300 m*M*[28] and maintains a fairly constatnt internal pH around 7.7.[29]

Yet one may ask the question if the helix-ring transition could be at least partially coupled directly by the membrane potential that controls ionic conditions. For a filament that responds to local ionic conditions, the triggering stimulus could be provided by ionic leaks accompanying changes in the membrane potential or by mechnoactive ion channels. The polymorphism we observed with FtsZ has remarkable similarities to bacterial flagella, which can adopt different conformations classified as straight filaments, helical filaments with different pitches and wave height as well as circular shapes with a very small pitch making it look similar to a toroid or small tube, depending on pH and ionic conditions (Ref. 30, plate XX). There are two possible mechanism which could lead to the observed polymorphism of FtsZ. Mechanism 1: FtsZ may be considered a chain of elastic subunits, where the preferred local conformation state of the filamentlike pitch or curvature is controlled by the local chemical conditions such as hydrolysis state of filament subunits or local ionic conditions which could effect the interaction between subunits. Thus, the local curvature and torsion of the FtsZ suprastructures would be dependant on the local chemical state. Mechanism 2: Individual FtsZ subunits can take on at least two different conformations and are bi-stable. Local conditions such as ionic conditions or pH could shift the bi-stable potential such that in the presence of potassium ions one conformation is energetically favored but in the presence of sodium ions the other state is favored. If FtsZ is entirely in one state and the ionic conditions shift such that the state is no longer energetically favored, then this will induce a flip in curvature or pitch as is seen in bacterial flagella. Mechanism 1 would produce an active motion of the suprastructure that is chemically driven at every point along its length, requiring only an ionic oscillation and a local flipping at one point to produce a wave motion. In Mechanism 2 the change of conformation will change the pitch resulting in traveling waves. FtsZ spirals observed in vivo showed periodic waves of oscillation with a periodicity of 30–60 s[8], thus favoring Mechanism 2. Yet, at present, not much is known about ionic fluctuations in bacterial cells.

What is the molecular structure and arrangement of the FtsZ filaments within the condensates we observed in the presence of molecular crowding? Crystal structures of FtsZ[31] suggested that FtsZ assembles in an orientation very similar to that observed for polymerized tubulin, with each FtsZ monomer maintaining head-to-tail interaction, forming a linear proto-filament. We obtained optical diffraction patterns from straight FtsZ bundles, which besides an equatorial reflection arising from weak liquid-like interfilament interactions gave rise to off

meridional reflections at a spacing of about 44 Å, its radial maximum being around 70 Å. As higher-order reflections on the equator were never observed, we concluded that filaments within the bundle adopted a random orientation relative to each other along the bundle long axis and the FT of a bundle would be the same as of a single filament spun around its axis.

The observation of an off meridional reflection indicated that the arrangement of monomers within the filaments observed in bundles were not straight but rather twisted or staggered proto-filament. Twisting could be directly observed when looking at FtsZ strands at the surface of bundles or toroids, which showed an appearance resembling single short or long pitch helices of F-actin (Figure 2d, supp. info., Figure 2f). Optical diffraction patterns of the long thin bundles formed with $BaCl_2$ also showed an off meridional reflection at about 45 Å with a radial peak at around 60 Å, also indicating that FtsZ monomers were twisted or stagered in these filaments rather than straight, although here a weak true meridional at about 42 Å could also be detected.

As the FtsZ toroids closely resembled those of DNA formed by multivalent cations such as Hexammine Cobalt or spermine published in the literature,[2] we studied the effects of multivalent cations on FtsZ. So far, only the effects of the divalent cation $CaCl_2$ have been extensively studied, and there are basically no studies using other cations. Adding $CaCl_2$ was shown to induce 2-D sheets consisting of pairs of parallel FtsZ proto-filaments forming a thick filament. Two thick filaments associated in an antiparallel fashion formed the unit cell. The effects of Hexammine Cobalt, spermine, and $BaCl_2$ on FtsZ gave novel results. All FtsZ condensates formed by these substances were entirely different from those observed with crowding agents. Especially, revealing were our observations on Hexammine Cobalt-induced FtsZ condensates. This trivalent cation induced a variety of novel 2-D sheets and tubes, with different proto-filament arrangement as in the $CaCl_2$ induced sheets. Crystalline tubes could also be obtained with FtsZ binding protein ZipA (supp. info., Figure 5), making Hexammine Cobalt-induced condensates good targets for further high resolution structural studies on the arrangement and conformation of *E. coli* FtsZ under various conditions and in the presence of binding proteins using cryo-EM or cryo-negative stain.

In summary, our results show that molecular crowding induces the unique FtsZ supramolecular structures like helices or rings observed in vivo, thus being a good example that one of the main predictions of crowding theory, which states that molecular crowding enhance native state stability is valid.[15,32] FtsZ filaments in these supramolecular structures appeared to be twisted rather than straight protofilaments. Transitions between helical, circular, or straight condensates[33] may result from both a structural change of the FtsZ monomer itself, although non has been observed so far,[31] or from structural changes of the intersubunit interface induced by ions, pH, or nucleotides. Polycations like Hexammine Cobalt induced an entirely different set of FtsZ suprastructures not found in vivo, which due to their novel crystalline arrangement may give us new insights on the structure and function of FtsZ and its associated proteins in the near future.

Supplementary Material

Refer to Web version on PubMed Central for supplementary material.

REFERENCES

1. Small JV, Rottner K, Kaverina I. Curr Opin Cell Biol 1999;11:54–60. [PubMed: 10047522]
2. Hud NV, Vilfan ID. Annu Rev Biophys Biomol Struct 2005;34:295–318. [PubMed: 15869392]
3. Levin PA, Losick R. Genes Dev 1996;10:478–488. [PubMed: 8600030]

4. Srinivasan R, Mishra M, Wu L, Yin Z, Balasubramanian K. Genes Dev 2008;22:1741–1746. [PubMed: 18593876]
5. Li Z, Trimble MJ, Brun YV, Jensen G. J EMBO J 2007;26:4694–4708.
6. Stricker J, Maddox P, Salmon ED, Erickson HP. Proc Natl Acad Sci USA 2002;99:3171–3175. [PubMed: 11854462]
7. Peters PC, Migocki MD, Thoni C, Harry E. J Mol Microbiol 2007;64:487–499.
8. Thanedar S, Margolin W. Curr Biol 2004;14:1167–1173. [PubMed: 15242613]
9. Tang JX, Janmey PA. J. Biol Chem 1996;271:8556–8563. [PubMed: 8621482]
10. Loewe J, Amos LA. EMBO J 1999;18:2364–2371. [PubMed: 10228151]
11. Lu C, Erickson HP. Methods Enzymol 1998;298:305–313. [PubMed: 9751890]
12. Moy FJ, Glasfeld E, Mosyak L, Powers R. Biochemistry 2000;39:9146–9156. [PubMed: 10924108]
13. Narita A, Maeda Y. J. Mol Biol 2007;365:480–501. [PubMed: 17059832]
14. Popp D, Gov NS, Iwasa M, Maeda Y. Biopolymers 2008;89:711–721. [PubMed: 18412138]
15. Minton AP. J Pharm Sci 2005;94:1668–1675. [PubMed: 15986476]
16. Popp D, Yamamoto A, Iwasa M, Maeda Y. Biochem Biophys Res Commun 2006;351:348–353. [PubMed: 17067551]
17. Zhao F, Craig R. J Struct Biol 2003;141:43–52. [PubMed: 12576019]
18. Gelbart WM, Bruinsma RF, Pincus PA, Parsegian VA. Phys Today 2000;53:38–44.
19. Oosawa, F. Polyelectrolytes. New York: Dekker; 1971.
20. Osawa M, Anderson DE, Erickson HP. Science 2008;320:792–794. [PubMed: 18420899]
21. Verwey, EJW.; Overbeek, JT. Theory of the Stability of Lyophobic Colloids: The Interaction of Sol Particles Having an Electric Double Layer. Amsterdam: Elsevier; 1948.
22. Scheffers D-J, den Blaaawen T, Driessen A. J M Mol Microbiol 2000;35:1211–1219.
23. Romberg L, Mitchison T. J Biochemistry 2004;43:282–288.
24. Mukherjee A, Lutkenhaus J. J Bacteriol 1994;176:2754–2758. [PubMed: 8169229]
25. Bramhill D, Thompson CM. Proc Natl Acad Sci USA 1994;91:5813–5817. [PubMed: 8016071]
26. Erickson HP, Taylor DW, Taylor KA, Bramhill D. Proc Natl Acad Sci USA 1996;93:519–523. [PubMed: 8552673]
27. Huecas S, Andreu JM. J Biol Chem 2003;278:46146–46154. [PubMed: 12933789]
28. Cayley S, Lewis BA, Guttman HJ, Record MT Jr. J Mol Biol 1991;222:281–300. [PubMed: 1960728]
29. Kashket ER. Biochemistry 1982;21:5534–5538. [PubMed: 6293545]
30. Oliva MA, Trambaiolo D, Loewe J. J Mol Biol 2007;373:1229–1242. [PubMed: 17900614]
31. Cheung MS, Klimov D, Thirumalai D. Proc Natl Acad Sci USA 2005;102:4753–4758. [PubMed: 15781864]
32. Oosawa, F.; Asakura, S. Thermodynamics of the Polymerization of Protein. London: Academic Press; 1975.
33. Gonzalez JM, Jimenez M, Velez M, Mingorance J, Andreu JM, Vicente M, Rivas G. J Biol Chem 2003;278:37664–37671. [PubMed: 12807907]

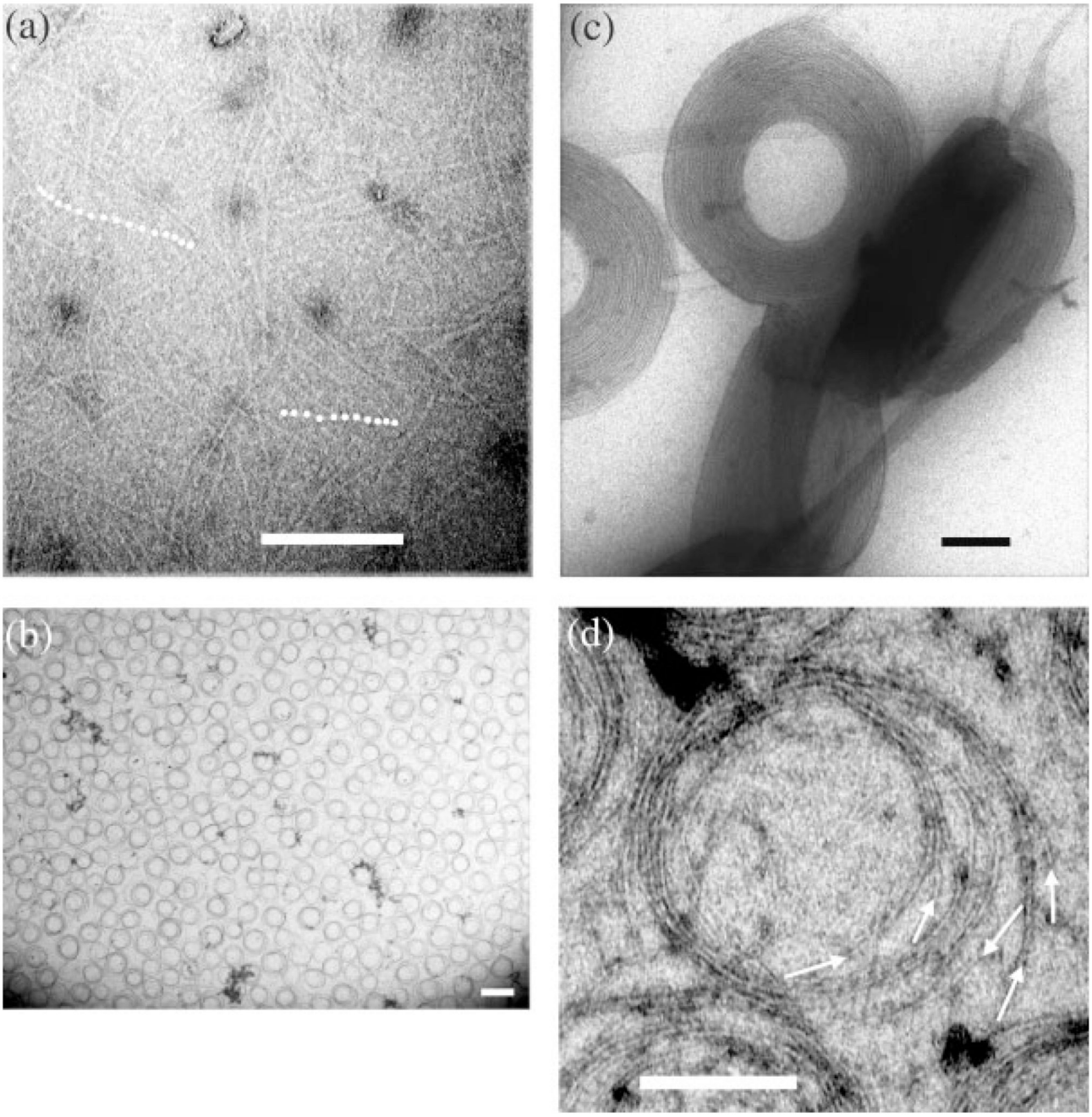

FIGURE 1.

Representative images of FtsZ filaments in the presence of various amounts of crowding agents, nucleotides, and KMg buffer. Results were pH independent (shown here pH 7.7, which is to the internal pH of *E. coli* in vivo). The appearance of the structures was similar with different crowding agents used, only the concentrations to induce the condensation phenomena differed between crowding agents. (a) FtsZ filaments below a critical concentration of crowding agent were mainly single filaments. Shown are FtsZ-GTP filaments in the presence of 0.4% MC highlighted as dotted lines, scale bar 100 nm. (b) Above the critical concentration, the equilibrium was shifted to rings consisting of several individual FtsZ filaments with an average diameter of about 220 nm. Shown are FtsZ-GTP filaments in the presence of 1.6% MC, scale

bar 500 nm. (c) Higher crowding agent concentrations (shown here FtsZ-GMPPNP in the presence of 8% PVA) condensed the structures into well defined toroids, scale bar 100 nm. (d) A closer look at the architecture of rings, which just started to condense above the critical concentration (shown at 1% MC). Individual filaments which form lateral contacts to neighboring filaments can be seen and the ends of individual filaments are marked with an arrow. Most filaments appeared to be between 400 and 800 nm long. Most rings observed consisted of single filaments, scale bar 100 nm.

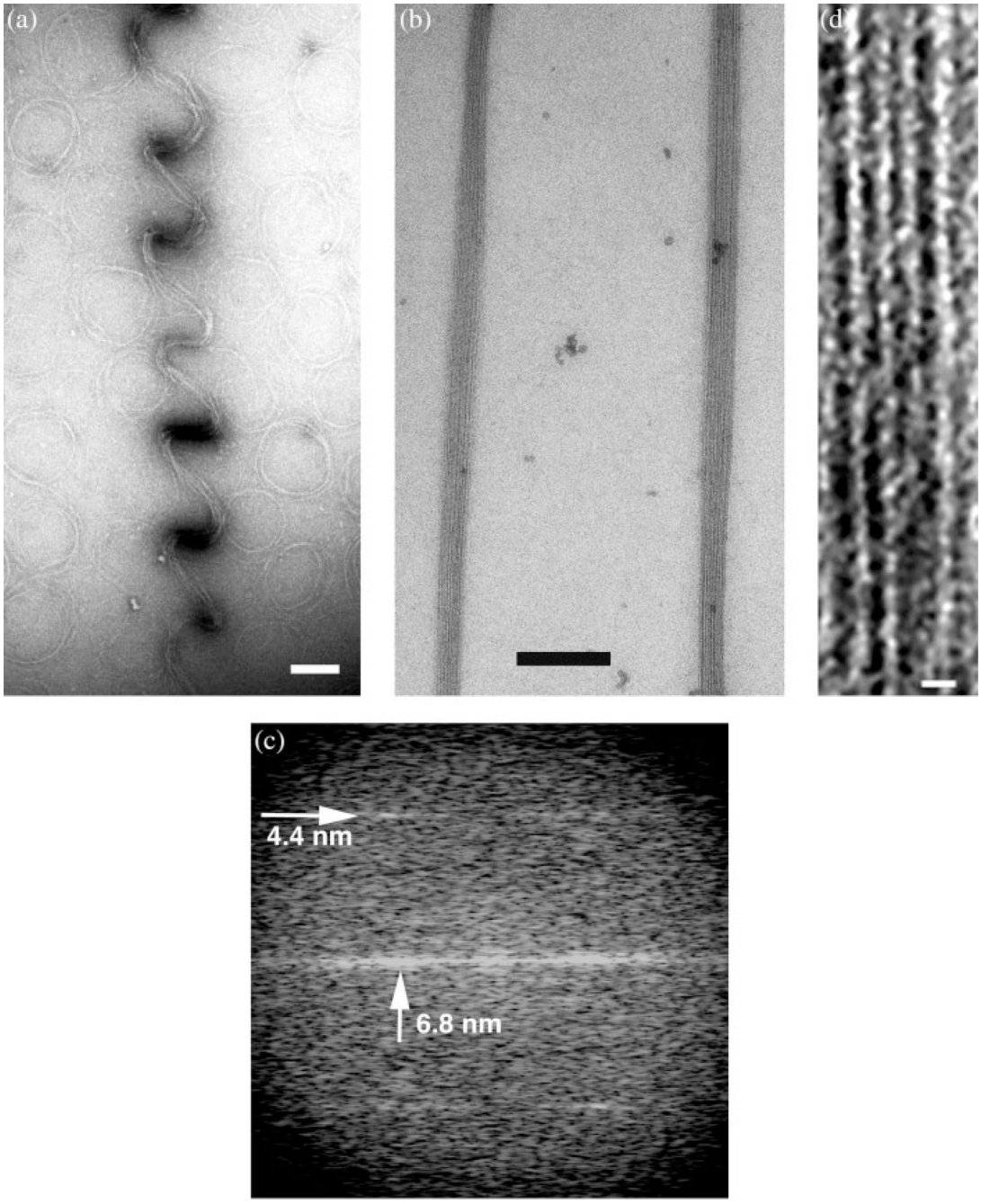

FIGURE 2.

Although the ring and toroid-like structures were predominant in all cases in KMg buffers in the presence of crowding agents above c_0, other structures were also observed. These structures could be observed with GTP or nonhydrolysable nucleotides and were independent of the type of crowding agent used. Shown here are representative images of other FtsZ-GTP suprastrutures (a) long multistranded helices with a pitch of about 300 nm and amplitude of about 200 nm (shown in the presence of 1.6% MC), scale bar 200 nm. (b) Long straight 3-D bundles (8% PVA), scale bar 200 nm. The outer filament layer of bundles or toroids was clearly visible when zooming in on some areas. (d) Shows the surface filaments of an FtsZ bundle. Note that the filaments do not appear to be straight proto-filaments; rather they seem to be

twisted, scale bar 5 nm. This is reflected by typical optical diffraction patterns of bundles (c) which give rise to two major reflections. An equatorial peak at about 6.8 nm arising from the side by side packing of FtsZ filaments and an off meridional reflection at about 4.4 nm, arising from the subunits in the filament forming a narrow spiral.

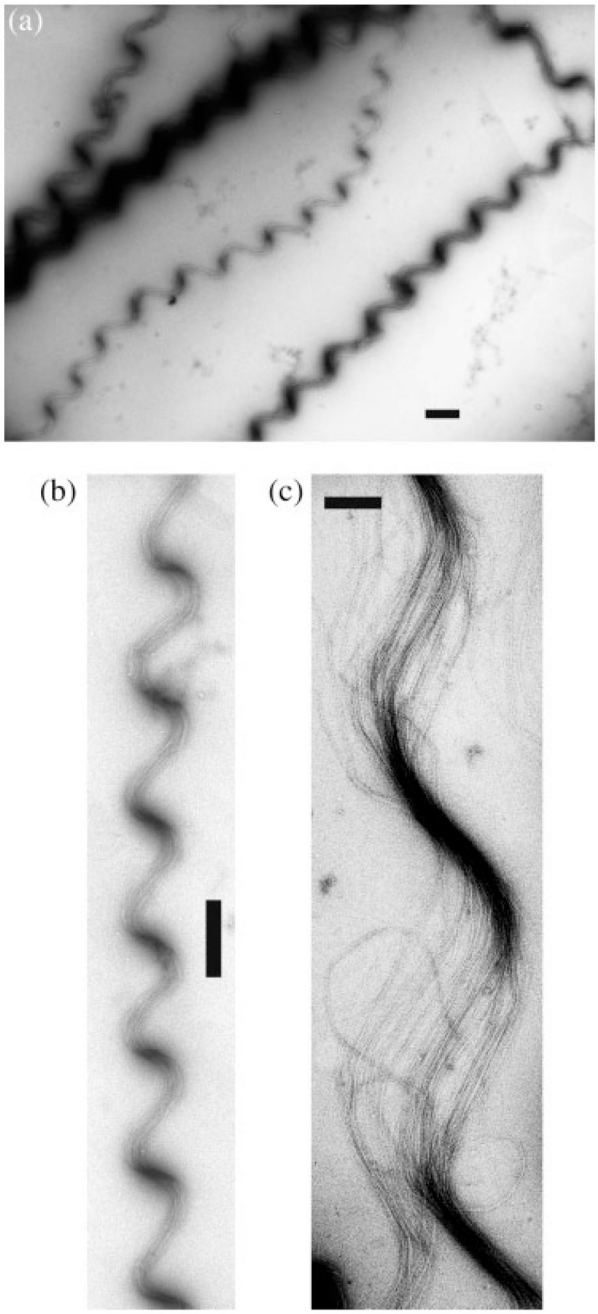

FIGURE 3.

Shown are the effects of EDTA on the formation of FtsZ suprastructures. KEDTA buffer was used together with crowding agents above c_0. (a) At pH to 6.6, only helical filaments were observed both with GTP and GMPPNP shown here FtsZ-GTP in the presence of 2% MC, scale bar 500 nm. (b) Closer views showed that the helices formed under these conditions were remarkably regular with a very long pitch around 780 nm and an amplitude of about 260 nm, scale bar 500 nm. (c) The architecture of these helical suprastructures becomes apparent when visualizing partially condensed spirals which were more common at low salt. Several μm long FtsZ filaments span the length of the helices and form lateral contacts with their neighbors, scale bar 100 nm.

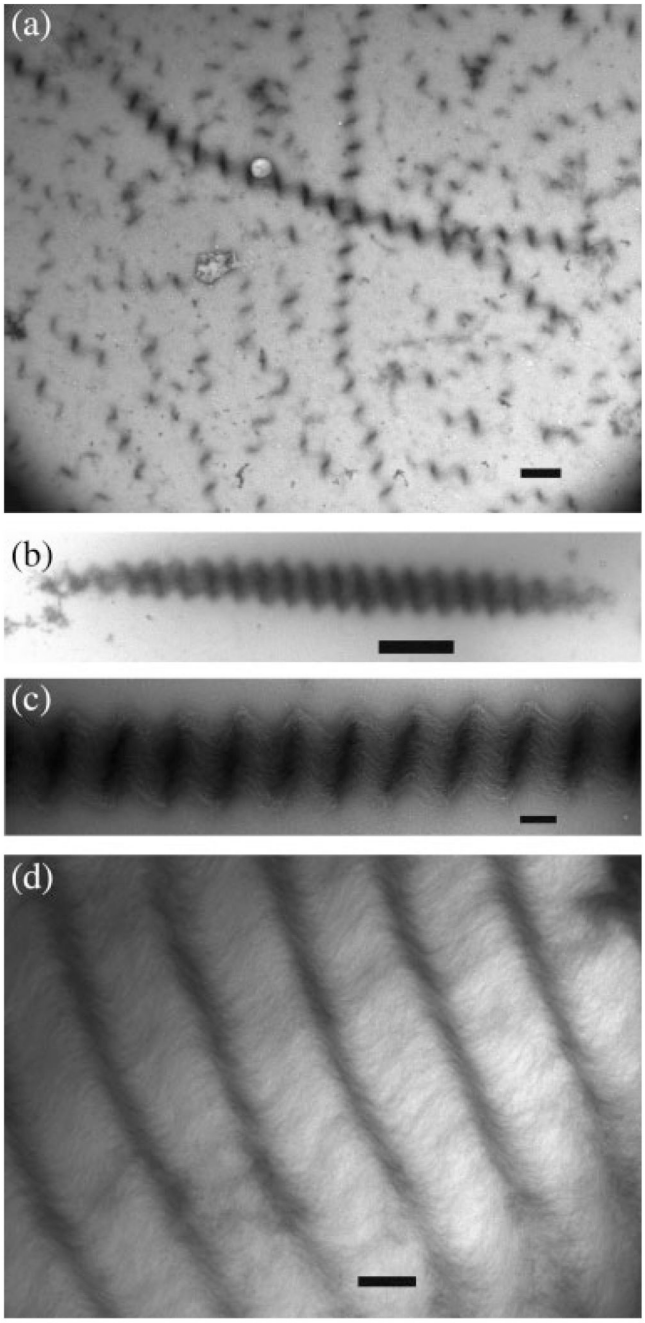

FIGURE 4.

Effect of sodium ions on the formation of FtsZ suprastructures. (a) In the presence of sodium and magnesium ions (NaMg buffer at both pH 6.6 and 7.7) and crowding agents above c_0, the majority species observed were helices. Both GTP and GMPPNP gave similar structures; the average pitch was around 390 nm with amplitude around 130 nm. Shown here FtsZ-GTP, 2% MC, pH 7.7 scale bar 500 nm. (b) Replacing Mg^{2+} ions by EDTA led to the formation of large spindle shaped suprastructures. These appeared independently of pH and for both GTP and GMPPNP. Shown here FtsZ-GTP, 2% MC, pH 6.6, scale bar 1 μm. (c) Closer inspection of these structures revealed that they are planar waves with a pitch of about 330 nm and an

amplitude of around 130 nm, scale bar 200 nm. (d) Planar waves could be up to several μm wide and very regular, scale bar 200 nm.

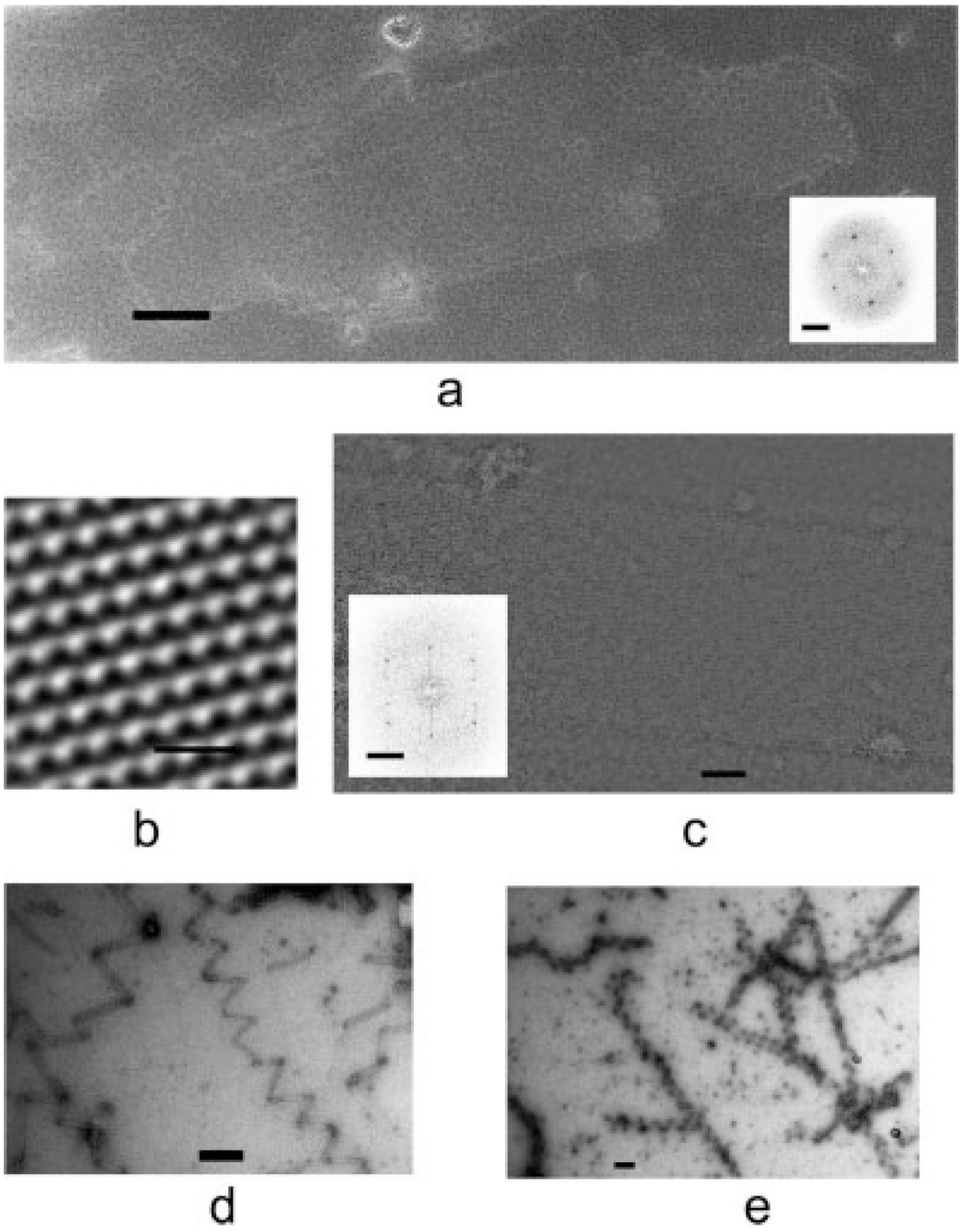

FIGURE 5.

FtsZ condensates formed by cations differed from those under crowed conditions. (a) Under low salt conditions and in the presence of magnesium ions and Hexammine Cobalt mostly 2-D crystals formed (scale bar 100 nm), which gave rise to a characteristic set of diffraction spots (insert, scale bar 5 nm). (b) Shows the averaged filtered projection structure with individual protofilaments running parallel to the long axis of the crystal, scale bar 10 nm. (c–e) In the presence of EDTA and Hexammine Cobalt, different condensates formed depending on the bound nucleotide. (c) In the presence of GDP, mainly large tubes formed, scale bar 100 nm, which gave an optical diffraction pattern with sharp spots (insert, scale bar 5 nm). (d) In the

presence of GTP, long helical ribbons formed, whereas in the presence of GMPPNP, (e) helical tubes were the predominant species, scale bars 200 nm.

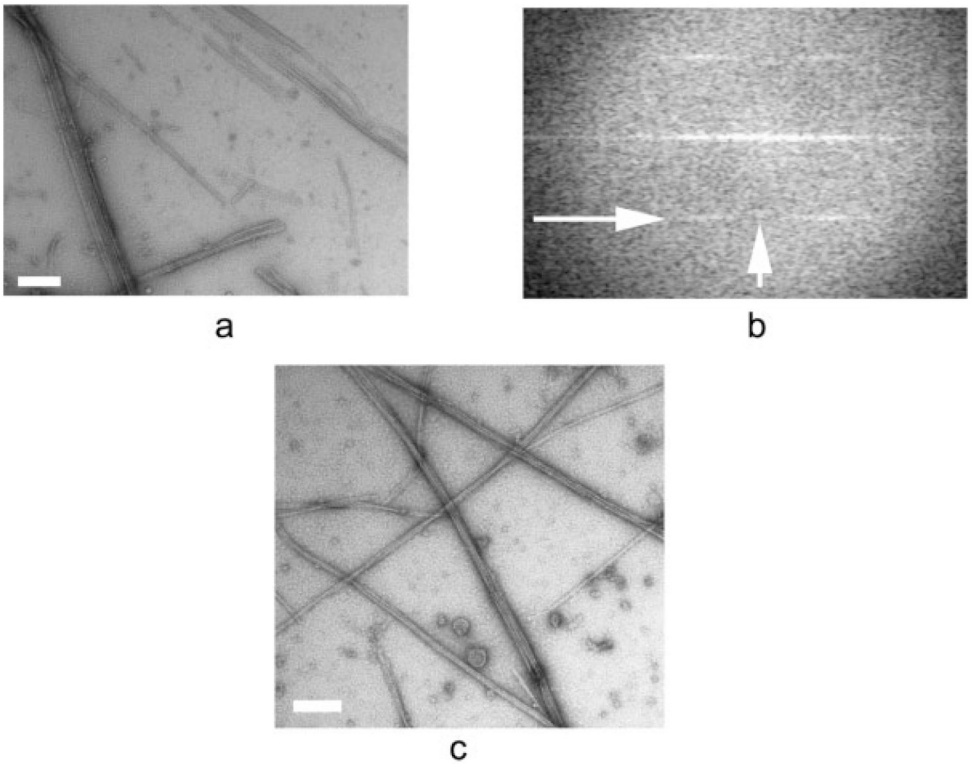

FIGURE 6.

In the presence of other cations, FtsZ formed long rafts, thin bundles, or rolled sheets. (a) With $BaCl_2$, the FtsZ suprastructures gave rise to a well-defined diffraction pattern shown in (b) A typical optical transform. Here, two clear reflections are visible, an off meridional reflection at about 45 Å and a weak meridional reflection at 42 Å, indicated by the arrows. (c) Spermine induced suprastructures where similar in appearance to those formed by $BaCl_2$, yet did not show a clear diffraction pattern, scale bars 200 nm.

Table I

Shown are Average Pitch and Amplitude Values Obtained From Helical and Planar Wave Condensates Under Various Conditions

Buffer Conditions	Helical/Wave Pitch (nm)	Helical/Wave Amplitude (nm)	Number of Structures Analyzed
KMg + CA, pH 6.6 and 7.7	300 ± 20	150 ± 15	10
KEDTA + CA, pH 6.6	780 ± 40	260 ± 30	30
NaMg + CA, pH 6.6 and 7.7	390 ± 30	130 ± 10	30
NaEDTA-buffer, pH 6.6 and 7.7	330 ± 20	130 ± 10	25

CA means crowding agent.